JOURNAL OF CATALYSIS **157**, 706–712 (1995)

The Role of the Mars and van Krevelen Mechanism in the Selective Oxidation of Nitrosobenzene and the Deoxygenation of Nitrobenzene on Oxidic Catalysts

E. J. Grootendorst, Y. Verbeek, and V. Ponec

Leiden Institute of Chemistry, Gorlaeus Laboratories, Leiden University, P.O. Box 9502, 2300 RA Leiden, The Netherlands

Received May 8, 1995; revised July 10, 1995; accepted July 18, 1995

The role of lattice oxygen atoms in the oxidation of nitrosobenzene to nitrobenzene has been established by using isotopically labeled oxides and, in other experiments, $^{18}O_2$ as oxidant. It appeared that with the most active catalyst, α-Mn_3O_4, the Mars and van Krevelen mechanism (oxidation by lattive oxygen atoms) is the most important mechanism. On γ-Fe_2O_3 and γ-Al_2O_3, disproportionation of nitrosobenzene prevails. © 1995 Academic Press, Inc.

INTRODUCTION

In general it is of great interest for modern technology to develop new waste-free or waste-lean processes. In particular stoichiometric reactions, like the removal of oxygen from an oxygen-containing molecule, are an example of reactions that are accompanied by a large production of waste. The batchwise production of 1 kg of nitrosobenzene from nitrobenzene by a stoichiometric reduction to phenylhydroxylamine followed by reoxidation to nitrosobenzene is accompanied by the production of 3 kg of salts (zinc and chromium) and diluted hydrochloric acid. These waste products are very hard to get rid of. A direct gas-phase reduction or deoxygenation of nitrobenzene to nitrosobenzene (and traces of aniline) is a much cleaner reaction (1–3) and is preferable to the stoichiometric reaction. Reduction or deoxygenation of carboxylic acids to aldehydes shows a similar picture and has to deal with the same problems.

The fundamental problems of selective deoxygenations are even more interesting than the practical ones. A nitrobenzene molecule or an anion of a carboxylic acid adsorbed on an oxide have two entirely equivalent oxygen atoms and nitrogen– or carbon–oxygen bonds. The fundamental question can be defined as follows: What is the mechanism of the selective removal of only one of these equivalent oxygen atoms?

In principle, two mechanisms are possible: (i) the molecule to be reduced is attacked by a reductant, both the molecule and the reductant being adsorbed on the surface (Langmuir–Hinshelwood mechanism) or (ii) the molecule is adsorbed on the catalyst surface, using an oxygen vacancy in the lattice of the oxide as a deposition place for one of its oxygen atoms (Mars and van Krevelen mechanism) (3). These two mechanisms are schematically shown in Fig. 1.

The idea that lattice oxygen atoms of an oxide appear in the products of both selective and deep oxidation reactions can be found already in the literature before World War II (4). Mars and van Krevelen (5) have derived the kinetic equations for this mechanism and have also proven it experimentally (6). In this mechanism a molecule (e.g., propene) picks up oxygen from the lattice of the oxidic catalyst, thereby creating an oxygen vacancy and acrolein. This vacancy is replenished by gaseous oxygen. In principle, this mechanism can also hold for selective deoxygenation reactions as illustrated in Fig. 1. The deoxygenation reactions of nitrobenzene (7) and aliphatic acids (8) have been studied in this respect. The results indicate that high selectivities to the desired products (nitrosobenzene and aldehydes) can be obtained and that this selectivity is due to the Mars and van Krevelen mechanism.

In this paper, isotopically labeled oxides are used to establish the role of the Mars and van Krevelen mechanism in the reactions of nitrosobenzene on oxides. To gain information about the transfer of oxygen between the molecules and oxidic catalysts, it is convenient to look at the selective oxidation of nitrosobenzene rather than the deoxygenation of nitrobenzene. When the oxidic catalyst has been labeled with ^{18}O atoms it is possible to follow the incorporation of lattice oxygen atoms in the desired product (nitrobenzene) and the total oxidation products CO and CO_2. This process is much easier to follow than the deposition of oxygen from an oxygen-containing molecule into the lattice of an

0021-9517/95 $12.00

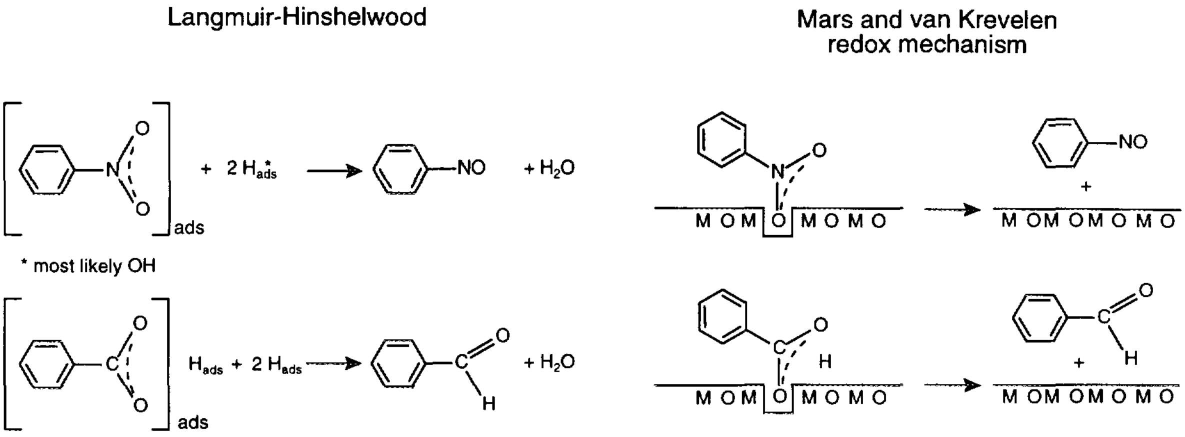

FIG. 1. Possible schematic pathways of deoxygenation reactions: via a Langmuir–Hinshelwood or a Mars and van Krevelen mechanism, i.e., with or without participation of lattice oxygen vacancies. (H_{ads} is most likely an OH-surface group.)

oxidic catalyst. In this way it can be established whether oxidation (both the selective and the total one) involves lattice oxygen or only oxygen originating from another nitrosobenzene molecule. With the principle of microscopic reversibility in mind one could extrapolate the results obtained for the selective oxidation to the selective deoxygenation reaction.

The selective oxidation of nitrosobenzene over a number of transition-metal oxides has been studied in a qualitative way. The most important results of this exploratory study are presented. Two transition-metal oxides, namely γ-Fe_2O_3 and α-Mn_3O_4, have been studied in more detail. Both oxides have been labeled with ^{18}O lattice oxygen atoms and the results of temperature-programmed reactions of nitrosobenzene on these oxides are presented.

METHODS

Preparation of the Catalysts Labeled with ^{18}O

α-Mn_3O_4 labeled with ^{18}O was prepared as follows. The oxide was first oxidized for 2 h at 573 K in flowing oxygen to remove carbon from the catalyst. Then the system was flushed with nitrogen. Subsequently, the catalyst was strongly reduced for 16 h at 648 K (α-Mn_3O_4). By this treatment MnO was formed. After the reduction the system was evacuated to 5.10^{-6} mbar, after which the catalyst was carefully reoxidized at 573 K with $^{18}O_2$ (Merck, Sharp and Dome Isotopes, 97.7% ^{18}O). The oxide prepared in this way should have an ^{18}O content of 33% ($MnO_1 \rightarrow MnO_{1.33}$). Iron oxide, γ-Fe_2O_3, was supplied by Technabexport (former USSR) through Delta Medical Scientific Instruments, Amsterdam. The enrichment in ^{18}O, roughly estimated from CO oxidation, was about 40% ^{18}O.

Prior to each experiment with these catalysts the system was evacuated for 16 h at 300°C. Any other pretreatment (if applied) is mentioned explicitly when describing the results.

Other Catalysts

In the first, exploratory part of the study, a number of oxides had been tested for their activity and selectivity in the oxidation of nitrosobenzene. The syntheses and origin of the oxides and their precursors are as follows.

V_2O_5 was prepared by decompositon of NH_4VO_3 (Baker Chemicals, Netherlands) in oxygen at 300°C for 6 h. Slowly heating $(NH_4)_2Cr_2O_7$ (Merck, Germany; *caution:* explosive decomposition!) to 200°C, followed by heating at 300°C for 2 h resulted in the formation of pure Cr_2O_3. Co_3O_4 was prepared by decomposition of $Co(NO_3)_2$ (Merck, Germany) in air: 24 h at 125°C, followed by 7 h at 500°C. Reduction of Co_3O_4 in hydrogen atmosphere at 250°C (17 h) resulted in CoO. Two different forms of PbO were synthesized. Red PbO (litharge) was prepared by heating $Pb(OH)_2$ (freshly prepared from $Pb(NO_3)_2$ and NH_4OH) in nitrogen at 575°C. Heating PbO_2 (Merck, Germany) for 1 h at 650°C in a nitrogen atmosphere resulted in yellow PbO (massicot).

Commercially available samples of TiO_2 (Eurotitania-1, TiOxide England) and γ-Al_2O_3 (Aluminiumoxid-C, Degussa Germany) were used as supplied. Table 1 shows the data of the different oxides, such as precursor, supplier, surface area, and XRD data.

Data Acquisition and Evaluation

A simple static apparatus, in which UHV pressures can be achieved, has been used throughout this study (9, 10). All experiments have been performed at total pressures lower than 1 mbar, to minimize mass transport problems. The apparatus was connected to a mass spectrometer, Fi-

TABLE 1

Relevant Data of the Investigated Oxides

Oxide	Precursor	Supplier	Area (m^2/g)	XRD	Bond strength (kJ/mol)
α-Mn_3O_4	$Mn(NO_3)_2 \cdot xH_2O$	Johnson Matthey	27	Pure	347.7
MnO	α-Mn_3O_4		—	—	387.4
V_2O_5	NH_4VO_3	Baker	11	Pure	319.6
Cr_2O_3	$(NH_4)_2Cr_2O_7$	Merck	36	Pure	383.1
Co_3O_4	$Co(NO_3)_2$	Merck	55	Pure	216.8
CoO	Co_3O_4		59	Traces Co_3O_4	238.1
PbO (red)	$Pb(OH)_2$		0.8	Pure	220.9
PbO (yellow)	PbO_2		0.8	Pure	217.7
TiO_2		Tioxide	47	Pure	477.7
γ-Al_2O_3		Degussa	95	Pure	563.6
γ-Fe_2O_3				Pure	278.9

sons Instruments MM8-80S with Nier-Johnson geometry, via a UHV dosing valve, Fisons Instruments MD6. The mass spectrometer was operated at low electron energy (25 eV) to avoid excessive fragmentation. The filament, suited for oxygen-rich atmospheres, was a commercially produced, ThO_2-coated iridium wire.

In a short explorative study, various oxides have been compared in a temperature-programmed reaction. The temperature was raised by 5°C/min and at two temperatures (125 and 250°C) a parameter called yield was evaluated:

$$\text{Yield} = \frac{I(C_6H_5NO_2)}{I(C_6H_5NO) + I(C_6H_5NO_2) + I(C_6H_5NH_2)},$$

where I stands for the intensity of the signals of the mass spectrometer. The mass-to-charge ratios used to monitor the reactions and in the figure legends throughout this paper have been tabulated in Table 2.

The temperature-programmed reactions have been performed with 2.5×10^{-2} mbar nitrosobenzene. In case of experiments in which a mixture of nitrosobenzene and oxygen are admitted to the system, the total pressure is 5×10^{-1} mbar (2.5×10^{-2} mbar nitrosobenzene and 47.5×10^{-1} mbar O_2). This is approximately a 20-fold excess of oxygen. Results shown in Figs. 3–9 are expressed in arbitrary units (a.u.). These units, when used in figures showing results for CO and CO_2 production should be multiplied by 10^3, to bring them into the same scale as used for selective oxidation products.

TABLE 2

Relation between Molecules and the *m/e* Ratios as Used in the Figure Legends

m/e ratio	Molecule	*m/e* ratio	Molecule	*m/e* ratio	Molecule
28	$C^{16}O$	44	$C^{16}O_2$	107	$C_6H_5N^{16}O$
30	$C^{18}O$	46	$C^{16}O^{18}O$	123	$C_6H_5N^{16}O_2$
32	$^{16}O_2$	48	$C^{18}O_2$	125	$C_6H_5H^{16}O^{18}O$
36	$^{18}O_2$	78	C_6H_6	127	$C_6H_5N^{18}O_2$

The average metal–oxygen bond strengths $-\Delta H^0$ were calculated from the heat of formation of the metaloxides ΔH_f as follows:

$$-\Delta H^0 = -\frac{1}{x}\Delta H_f(MO_x) = -\frac{1}{x}\frac{1}{y}\Delta H_f(M_yO_{xy}).$$

The calculated metal–oxygen bond strengths can be found in Table 1.

RESULTS

A. A Comparison of the Reactivity of Various Metal Oxides

Based on temperature-programmed reactions (TPR) of nitrosobenzene (experiments without molecular oxygen in the gas phase) a rough estimate has been made of the reactivities of various metal oxides. To eliminate the influence of the amount of catalyst on the reactivity, the parameter yield has been normalized per unit surface area of the catalyst (Fig. 2).

It can be seen that not all oxides show activity for the selective oxidation of nitrosobenzene. V_2O_5 showed only activity for oxidation/decomposition to CO, while PbO (yellow and red), CoO, and TiO_2 showed no activity at all throughout the whole temperature range (25–300°C). If total oxidation to CO_2 (not shown in the figure) took place, this always happened at temperatures higher than the temperature at which the selective oxidation occurred (total oxidation temperature ≥250°C).

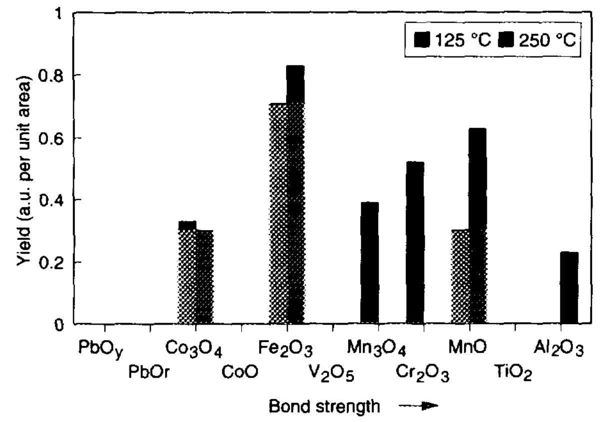

FIG. 2. Yield of nitrobenzene plotted in the sequence of increasing bond strength (calculated from the heat of formation of the various oxides). The nominal composition of the catalysts at the steady state of the reaction has been indicated.

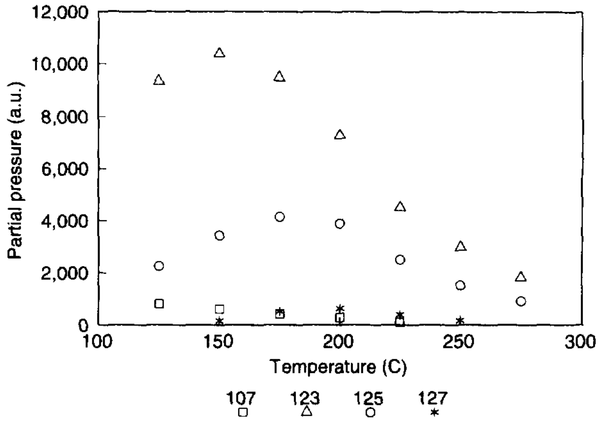

FIG. 4. Formation of selective oxidation products on α-$Mn_3{}^{18}O_4$, partial pressures (in arbitrary units), as a function of temperature (TPR mode).

B. TPR of Nitrosobenzene on ^{18}O Labeled α-Mn_3O_4

Figures 3 and 4 show the results of the temperature-programmed reaction of nitrosobenzene over α-Mn_3O_4 labeled with ^{18}O atoms. The partial pressures on the y-axis are in arbitrary units (i.e., the mass spectrometer intensities have not been corrected for relative sensitivities).

Formation of nitrobenzene (m/e = 123: no ^{18}O atom and m/e = 125: one ^{18}O atom per molecule) takes place at temperatures between 75 and 200°C. The total oxidation (destruction of the C_6 ring) occurs at temperatures higher than 225°C. All isotopically labeled forms of CO and CO_2 have been formed at 300°C. Figure 4 has an enlarged scale compared with Fig. 3. The sensitivity of the detector of the mass spectrometer (secondary electron multiplier) has been increased to follow also the formation of nitrobenzene with m/e = 127 (two ^{18}O atoms). The figure clearly shows that this isotopically labeled molecule has been formed too.

Figures 5 and 6 show the results of temperature-programmed experiments of a mixture of nitrosobenzene and $^{16}O_2$ and ^{18}O-labeled α-Mn_3O_4. These experiments have been performed in order to determine whether the presence of $^{16}O_2$ in the gas phase influences the product/isotope distribution as obtained without $^{16}O_2$ in the gas phase (Figs. 3 and 4). The temperature has been raised to 200°C and was then kept constant.

The arrows at the top of Figs. 5 and 6 indicate the moment at which $^{16}O_2$ has been introduced into the gas phase. With a rising temperature the concentration of $^{16}O_2$ decreased rapidly to zero (not shown in the figures). Therefore, a second dose of $^{16}O_2$ had to be admitted. All selective oxidation products (i.e., all isotopically labeled molecules)

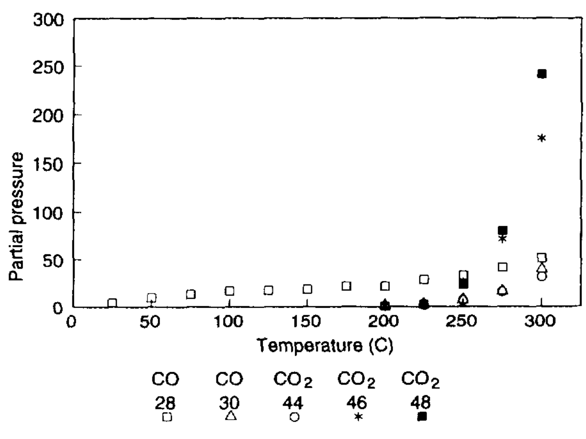

FIG. 3. Formation of total oxidation products on α-$Mn_3{}^{18}O_4$, partial pressure (in arbitrary units), as a function of temperature (TPR mode).

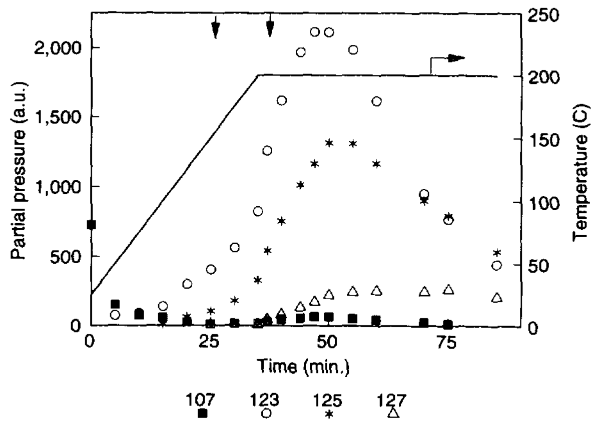

FIG. 5. Formation of selective oxidation products on α-$Mn_3{}^{18}O_4$ (with $^{16}O_2$ in the gas phase), partial pressures (in arbitrary units), as a function of time.

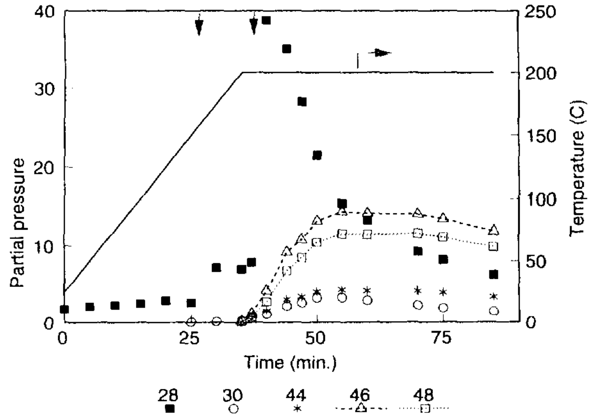

FIG. 6. Formation of total oxidation products on α-$Mn_3{}^{18}O_4$ (with $^{16}O_2$ in the gas phase), partial pressure (in arbitrary units), as a function of time.

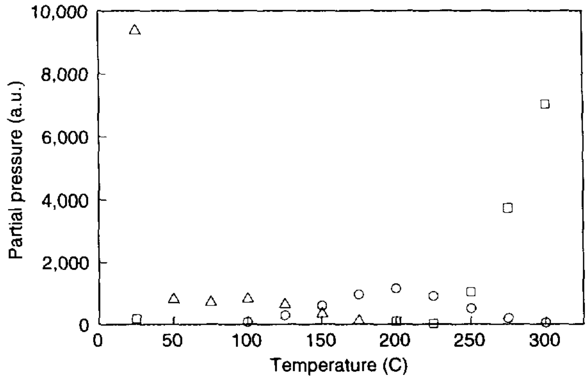

FIG. 8. Formation of selective oxidation products on γ-$Fe_2{}^{18}O_3$, partial pressure (in arbitrary units), as a function of temperature (TPR mode). (□) Benzene, mass 78; (△) nitrosobenzene, mass 107; (○) nitrobenzene, mass 123.

have been formed during the experiments (Fig. 5). The product distribution is not different from the one shown in Figs. 3 and 4. The same can be said about the product distribution of the total oxidation products. Carbon monoxide is the only product which is influenced by admitting $^{16}O_2$. After admitting oxygen the concentration of CO increases strongly, but with increasing time the concentration of CO decreases again.

C. TPR of Nitrosobenzene on ^{18}O Labeled γ-Fe_2O_3

In Figs. 7 and 8 the results of the temperature-programmed reaction of nitrosobenzene on γ-Fe_2O_3 labeled with ^{18}O atoms are shown. Figure 7 shows the partial pressures of the total oxidation products formed, while Fig. 8 shows the formation of the selective oxidation products (both as a function of temperature).

It can be seen that only nitrobenzene with $m/e = 123$ (i.e., without ^{18}O atoms) has been formed. Increasing the sensitivty of the detector does not result in the detection of other, isotopically labeled, forms of nitrobenzene. Nitrobenzene is formed between 100 and 200°C. At temperatures higher than 225°C, benzene can also be detected in the gas phase. Figure 7 shows that ^{18}O atoms from the lattice can be incorporated in the total oxidation product CO_2 (in contrast to the formation of nitrobenzene). All three possible forms ($C^{16}O_2$, $C^{16}O^{18}O$, and $C^{18}O_2$) are formed at temperatures higher than 225°C.

Figure 9 shows the results of the temperature-programmed reaction of a mixture of nitrosobenzene and $^{18}O_2$ in the gas phase with γ-Fe_2O_3 (not labeled) as a catalyst. Nitrobenzene is formed between 100 and 200°C; above this temperature its concentration decreases again due to total oxidation and decomposition. A small amount of $C_6H_5N^{16}O^{18}O$ ($m/e = 125$) can also be detected. In this experiment the maximum signal intensity of this product

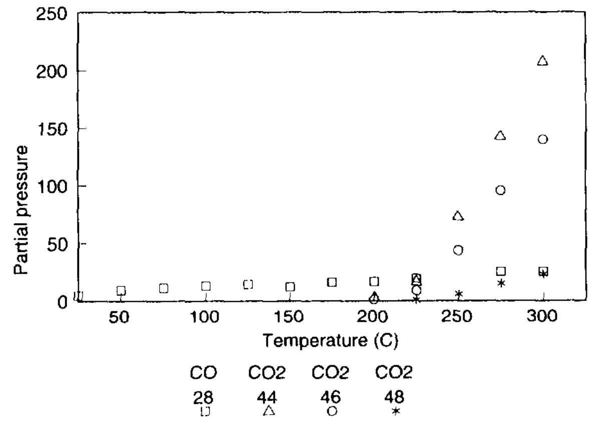

FIG. 7. Formation of total oxidation products on γ-$Fe_2{}^{18}O_3$, partial pressure (in arbitrary units), as a function of temperature (TPR mode).

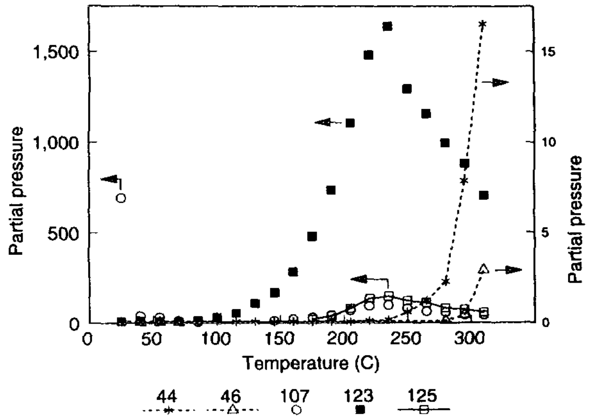

FIG. 9. Temperature-programmed reaction of C_6H_5NO + $^{18}O_2$ on γ-Fe_2O_3 (unlabeled); partial pressures vs temperature.

is about 10% of the intensity of unlabeled nitrobenzene. The concentration of $^{18}O_2$ in the gas phase is not shown in the figure. Up until 175°C the concentration of $^{18}O_2$ was very high, but between 175 and 190°C the gas-phase concentration decreased very fast to zero. Both $C^{16}O_2$ and $C^{16}O^{18}O$ are formed at temperatures higher than 225°C. The concentration of $C^{16}O^{18}O$ ($m/e = 46$) is about 20% of the concentration of $C^{16}O_2$ ($m/e = 44$). $C^{18}O_2$ is not formed or its concentration is too low to be measured.

DISCUSSION

The estimation of the activity of several oxides for the oxidation of nitrosobenzene revealed that the oxides with the highest and the lowest metal–oxygen bond strength are not active in the selective oxidation of nitrosobenzene to nitrobenzene. Several authors predict such a correlation (11–13). However, it would be very premature to make any conclusion at this stage of discussion. The most interesting result namely is that the mechanism of oxidation is substantially different on different oxides, as can be seen below.

The reactions on α-Mn_3O_4 clearly are of the Mars and van Krevelen type. Lattice oxygen atoms (^{18}O) appear in the products of both the selective ($C_6H_5N^{16}O^{18}O$) and the total, destructive oxidation of nitrosobenzene ($C^{18}O$, $C^{16}O^{18}O$, $C^{18}O_2$). Double labeled nitrobenzene ($C_6H_5N^{18}O_2$) is also formed. This product can be formed from either a consecutive oxygen exchange reaction of nitrobenzene or a product of the following reaction: $C_6H_5N_{ads} + 2\ ^{18}O_{lattice}$.

The first explanation of the formation of $C_6H_5N^{18}O_2$ can be excluded. Adsorption of unlabeled nitrobenzene on α-Mn_3O_4 labeled with ^{18}O-lattice atoms between 150 and 300°C did not result in the formation of any molecule of nitrobenzene labeled with ^{18}O. Thus it could be concluded that the formation of $C_6H_5N^{18}O_2$ is not the result of a consecutive oxygen exchange reaction.

The intermediate $C_6H_5N_{ads}$ can be formed by direct dissociation,

$$C_6H_5NO_{ads} \rightarrow C_6H_5N_{ads} + O_{ads},$$

or by disproportionation in the adsorbed state,

$$2(C_6H_5NO_{ads}) \rightarrow C_6H_5NO_2 + C_6H_5N_{ads}.$$

In the latter case, nitrobenzene is formed without participation of lattice oxygen atoms by a Langmuir–Hinshelwood mechanism.

On γ-Al_2O_3 it is not very likely that oxidation reactions occur via a Mars and van Krevelen mechanism and the formation of nitrobenzene is a result of a reaction among adsorbed molecules of nitrosobenzene. By studying the adsorption of nitrosobenzene on alumina with FTIR spectroscopy, Angevaare (14) and Koutstaal *et al.* (15) have shown that the appearance of nitrobenzene in the gas phase is accompanied by the formation of azoxybenzene in the adsorbed state. Azoxybenzene can be formed by a reaction between two nitrosobenzene molecules.

TABLE 3

Relative Presence (in %) of Labeled Products in the Gas Phase

T(°C):	125	150	175	200	225	250	275	300
44				25	19	12	9	7
46				59	52	46	43	39
48				16	29	42	48	54
123	81	74	67	62	61	64	66	
125	19	25	29	33	34	32	34	
127	0	1	4	5	5	4	0	

On iron oxide the results are similar to those on alumina, although iron oxide has a higher activity; nitrobenzene is formed already at 125°C. The formation of nitrobenzene on γ-Fe_2O_3 occurs without detectable participation of lattice oxygen atoms and is a sole result of the reaction between nitrosobenzene molecules in the adsorbed state. However, the total, destructive oxidation of nitrosobenzene does occur with lattice oxygen atoms (see Fig. 7). It can be stated at this point that the oxidation of nitrosobenzene to nitrobenzene on γ-Fe_2O_3 by lattice oxygen atoms is considerably slower than the oxidation by oxygen from another nitrosobenzene molecule.

To complete this information, a temperature-programmed reaction of nitrosobenzene on unlabeled γ-Fe_2O_3 has been performed in the presence of $^{18}O_2$ in the gas phase. As can be seen from Fig. 9, unlabeled nitrobenzene (m/e ratio = 123) is the major product, while only a small amount of ^{18}O is incorporated (resulting in $C_6H_5N^{16}O^{18}O$). The disproportionation of nitrosobenzene is obviously faster than the oxidation by ^{18}O adsorbed on the catalyst from the gas phase. Activated adsorption of $^{18}O_2$ is evidenced by the pressure drop between 170 and 190°C (as described under Results). Oxygen is adsorbed on the surface and probably incorporated in the lattice at specific sites. It can be seen in Fig. 9 that ^{18}O does appear in CO_2 (namely $C^{16}O^{18}O$), although not to a great extent.

Concerning the selective oxidation of nitrosobenzene it can be concluded that the reactivity of lattice oxygen atoms is in the following order: α-$Mn_3O_4 \gg \gamma$-$Fe_2O_3 > \gamma$-Al_2O_3.

On α-Mn_3O_4, the Mars and van Krevelen mechanism is undoubtedly the most important mechanism with regard to both the selective and destructive oxidation of nitrosobenzene. However, a closer inspection of the results reveals more details. Table 3 shows the relative isotopic composition of the products in the gas phase at different temperatures during a TPR experiment (the relative isotopic composition is calculated as the intensity of one isotopically labeled product divided by the total of the intensities of all isotopically labeled products times 100). At approximately 200°C, the isotope distribution in nitrobenzene approaches the ^{18}O isotopic content in α-Mn_3O_4 ($\approx$33% ^{18}O in α-Mn_3O_4). At temperatures lower than 200°C, $C_6H_5N^{16}O_2$ has been formed preferentially. The relative occurrence of $C_6H_5N^{16}O_2$ is approximately 15–20% higher than the equilibrium composition. It is most likely that at these temperatures a small part of the selective oxidation takes place via the Langmuir–Hinshelwood reaction mentioned before, i.e., via a reaction in the adsorbed phase. However, the major part of nitrobenzene has been formed by the Mars and van Krevelen mechanism as reflected by the formation of $C_6H_5N^{16}O^{18}O$ at low temperatures. This product can only be a result of an oxidation by lattice oxygen atoms.

As already mentioned in the results, the isotopic composition of nitrobenzene is not greatly influenced by the presence of $^{16}O_2$ in the gas phase. When performing the same data analysis as above, we found that at 200°C the relative presence of $C_6H_5N^{16}O^{18}O$ is 28% instead of the expected 33%. Some oxides active in the reduction of nitrobenzene are not active in the oxidation of nitrosobenzene and, at first glance, it seems that the principle of microscopic reversibility is violated here. However, it is not. Reduction of nitrobenzene occurs at temperatures at which the phenyl ring can extract oxygen from the lattice, whereas nitrosobenzene does not have sufficient reactivity to oxygen to do that.

CONCLUSIONS

1. Nitrobenzene can be formed from nitrosobenzene by two different reaction mechanisms: (i) a reaction mechanism involving lattice oxygen atoms (the so-called Mars and van Krevelen mechanisms) and (ii) a disproportionation reaction (Langmuir–Hinshelwood).

2. The reactivity of lattice oxygen atoms and the participation of these oxygen atoms in the selective oxidation of nitrosobenzene follows the order: α-$Mn_3O_4 \gg \gamma$-$Fe_2O_3 \geq \gamma$-Al_2O_3. On α-Mn_3O_4, the Mars and van Krevelen mechanism is the most important one (>80%), while on γ-Fe_2O_3 the disproportionation mechanism takes place almost solely.

3. Oxidation of nitrosobenzene to CO and CO_2 (total, destructive oxidation) almost solely involves oxidation by means of lattice oxygen atoms on both α-Mn_3O_4 and γ-Fe_2O_3.

REFERENCES

1. Dodman, D., Pearson, K. W., and Woolley, J. M., *Brit. Appl.* 1,322,531 (1973).
2. Zengel, H. G., and Bergfeld, M., *Ger. Offen* 2,939,692 (1981).
3. Favre, T. L. F., Seijsener, P. J., Kooyman, P. J., Maltha, A., Zuur, A. P., and Ponec, V., *Catal. Lett.* **1,** 457 (1988).
4. Kröger, C., *Z. Anorg. Allg. Chem.* **206,** 289 (1932).
5. Mars, P., and van Kreelen, D. W., *Chem. Eng. Sci.* **3,** 41 (1954).
6. Mars, P., and Maessen, J. G. H., *in* "Proceedings, 3rd International Congress on Catalysis, Amsterdam, 1964" (W. M. H. Sachtler, G. C. A. Schuit, and P. Zwietering, Eds.), Vol. 1, p. 266. Wiley, New York, 1965.
7. Maltha, A., van Wermeskerken, S. C., Favre, T. L. F., Angevaare, P. A. J. M., Grootendorst, E. J., Koutstaal, C. A., Zuur, A. P., and Ponec, V., *Catal. Today* **10,** 387 (1991).
8. Grootendorst, E. J., Pestman, R., Koster, R. M., and Ponec, V., *J. Catal.* **148,** 261 (1994).
9. Van der Plank, P., and Sachtler, W. M. H., *J. Catal.* **12,** 35 (1968).
10. Grootendorst, E. J., Thesis, Leiden University, The Netherlands, 1994.
11. Haber, J., *Z. Chem.* **13,** 247 (1973).
12. Roiter, V. A., Golodets, G. I., and Pyatnitzkii, Yu.I., *in* "Proceedings, 4th International Congress on Catalysis, Moscow, 1968" (B. A. Kazansky, Ed.), Vol. 1, p. 466. Akademiai Kiado, Budapest, 1971.
13. Golodets, G. I., *in* "New Developments in Selective Oxidation" (G. Centi and F. Trifiro, Eds.), Studies in Surface Science and Catalysis 55, p. 693. Elsevier, Amsterdam, 1990.
14. Angevaare, P. A. J. M., Ph.D. thesis, Leiden University, 1991.
15. Koutstaal, C. A., Angevaare, P. A. J. M., Grootendorst, E. J., and Ponec, V., *J. Catal.* **141,** 82 (1993).